BSAVA BRITISH SMALL ANIMAL VETERINARY ASSOCIATION

PAPER

Radiographic and ultrasonographic findings of the spleen and abdominal lymph nodes in healthy domestic ferrets

J. N. Suran*[,1], L. V. Latney* and N. R. Wyre[†]

*Department of Clinical Studies, School of Veterinary Medicine, University of Pennsylvania, Philadelphia, PA, 19104, USA
[†]Zodiac Pet & Exotic Hospital, Tin Hau, Hong Kong

[1]Corresponding author email: jsuran@vet.upenn.edu

Objective: To describe the radiographic and ultrasonographic characteristics of the spleen and abdominal lymph nodes in clinically healthy ferrets.

Materials and Methods: Fifty-five clinically healthy ferrets were prospectively recruited for this cross-sectional study. Three-view whole body radiographs and abdominal ultrasonography were performed on awake (23 out of 55) or sedated (32 out of 55) ferrets. On radiographs splenic and abdominal lymph node visibility was assessed. Splenic thickness and echogenicity and lymph node length, thickness, echogenicity, number and presence of cyst-like changes were recorded.

Results: The spleen was radiographically detectable in all ferrets. On ultrasound the spleen was hyperechoic to the liver (55 out of 55) and mildly hyperechoic (28 out of 55), isoechoic (15 out of 55) or mildly hypoechoic (12 out of 55) to the renal cortices. Mean splenic thickness was 11.80 ±0.34 mm. Lymph nodes were radiographically discernible in 28 out of 55 ferrets and included caudal mesenteric and sublumbar nodes. An average of 9 ±2 lymph nodes (mean± standard deviation; mode 10) were identified in each ferret using ultrasound. A single large jejunal lymph node was identified in all ferrets and had a mean thickness of 5.28 ± 1.66 mm. For other lymph nodes the mean thickness measurements plus one standard deviation were less than 4.4 mm (95% confidence interval: ≤ 3.72 mm).

Clinical Significance: The information provided in this study may act as a baseline for evaluation of the spleen and lymph nodes in ferrets.

Journal of Small Animal Practice (2017) **58**, 444–453
DOI: 10.1111/jsap.12680

Accepted: 7 March 2017; Published online: 17 April 2017

INTRODUCTION

Radiography and ultrasonography are part of the standard of care in domestic ferrets; however, there are few reports describing imaging findings or anatomic variations, despite lymph node lesions such as reactive lymphadenopathy and lymphoma occurring commonly in ferrets (O'Brien *et al.* 1996, Paul-Murphy *et al.* 1999, Schwarz *et al.* 2003, Kuijten *et al.* 2007, Zaffarano 2010, Garcia *et al.* 2011, Eshar *et al.* 2013, Mayer *et al.* 2014). Radiographic and ultrasonographic references provide a baseline for clinical evaluations.

In ferrets, there is a large jejunal lymph node in the mid-abdomen at the root of the mesentery which is commonly palpable in healthy individuals (Paul-Murphy *et al.* 1999). The jejunal lymph node is also known as the mesenteric lymph node or cranial mesenteric lymph node. According to the *Nomina Anatomica Veterinaria* (WAVA-ICVGAN 2012), while the jejunal lymph nodes are part of the cranial mesenteric lymphocentre, carnivores lack a cranial mesenteric lymph node. Therefore, although historically this lymph node has been identified as the

Presented in abstract form at the 2015 American College of Veterinary Radiology annual scientific conference in Minneapolis, MN and at the 2014 Association of Exotic Mammal Veterinarians annual scientific conference in Orlando, FL.

JSAP JOURNAL OF SMALL ANIMAL PRACTICE

mesenteric lymph node, it may be more appropriately termed the jejunal lymph node in ferrets, and will be referred to as such throughout this article. In both previous studies evaluating ferret lymph nodes with ultrasound, a single large jejunal lymph node was found in all animals (Paul-Murphy *et al.* 1999, Garcia *et al.* 2011). With ultrasound, the jejunal lymph node was described as a round to ovoid structure with uniform echogenicity near the centre of the small intestinal mesentery and near the cranial and caudal mesenteric veins surrounded by fat (Paul-Murphy *et al.* 1999). The mean and standard deviation for mesenteric lymph node dimensions varied somewhat between the studies and was reported as 7·6 ±2·0 mm thick by 12·6 ±2·6 mm long and 5·3 ±1·39 mm thick by 10·18 ±2·36 mm long (Paul-Murphy *et al.* 1999, Garcia *et al.* 2011).

In the later of the two ultrasound studies, the pancreaticoduodenal, splenic, gastric and hepatic lymph nodes were also examined (Garcia *et al.* 2011). Anatomic landmarks for those lymph nodes were similar to that previously described in cats (Schreurs *et al.* 2008). Pancreaticoduodenal lymph nodes were identified in 55%, splenic lymph nodes in 55%, gastric lymph nodes in 20% and hepatic lymph nodes in 5% of the 20 ferrets (Garcia *et al.* 2011). Lymph nodes were described as circular to elongate, hypoechoic structures surrounded by fat; some lymph nodes also had a faint echogenic halo. Length measurements (mean ±standard deviation) for the pancreaticoduodenal lymph nodes were reported as 5·29 ±1·32 mm, for the gastric lymph nodes as 7·7 ±2·6 mm, and for the splenic lymph nodes as 5·93 ±1·59 mm; thickness measurements were only provided for the mesenteric lymph node (Garcia *et al.* 2011).

In dogs and cats these and several other lymph nodes, such as the colic and medial iliac nodes, can be detected with ultrasound (d'Anjou 2008, Schreurs *et al.* 2008). Whether all of the lymph nodes detected in other carnivore species could be ultrasonographically identified in ferrets has not been determined.

While splenomegaly is common in ferrets, the imaging appearance of the spleen in clinically healthy ferrets has also not been previously described. Potential causes for splenomegaly include extramedullary haematopoiesis, neoplasia (especially lymphoma), lymphoid or myeloid hyperplasia, hypersplenism and infectious diseases such as Aleutian disease, systemic coronavirus infection, mycobacteriosis and cryptococcus (Ferguson 1985, Eshar *et al.* 2010, Dominguez *et al.* 2011, Morrisey & Kraus 2012, Pollock 2012, Mayer *et al.* 2014, Nakata *et al.* 2014, Lindemann *et al.* 2016). The spleen also increases in size with age and after administration of anaesthetics (Fox 2014, Mayer *et al.* 2014).

The goal of this prospective, cross-sectional study was to describe the characteristics of the spleen and abdominal lymph nodes on radiographs and with ultrasound in a sample of client-owned, clinically healthy domestic ferrets (*Mustela putorius furo*).

MATERIALS AND METHODS

Healthy, client-owned ferrets between four months and four years of age were prospectively recruited at the Matthew J Ryan Veterinary Hospital of the University of Pennsylvania between February 2013 and October 2013. For the calculation of sample sizes, the standard deviations of previously reported measurements of abdominal viscera in clinically healthy ferrets were compared, including gross renal measurements (1·25, 1·5 mm), ultrasonographic adrenal thickness (0·5, 0·6 mm) and ultrasonographic jejunal lymph node thickness (1·39, 2.0 mm) (O'Brien *et al.* 1996, Paul-Murphy *et al.* 1999, Kuijten *et al.* 2007, Garcia *et al.* 2011, Krautwald-Junghanns *et al.* 2011, Fox 2014). Using an averaged standard deviation for adrenal gland thickness of 0·55 mm and 90 to 95% confidence intervals (CI) of ±0·25 mm, the number of individuals needed to detect significant differences in organ measurements would be 14 (90% CI) to 19 (95% CI) (Hulley 2007). Using an averaged standard deviation of the renal measurements (1·375 mm) and 90 to 95% CI of ±0·6 mm gives the same results (Hulley 2007). These standard deviation values were chosen because of the relatively small differences in the respective reported values. As adrenal and renal size has been shown to vary based on sex, we estimated that a total of 19 ferrets for each sex would be needed, requiring a total recruitment of at least 38 clinically healthy ferrets (Neuwirth *et al.* 1997, Eshar *et al.* 2013). Additional ferrets were able to be enrolled because of the success of recruitment and remaining funding. This study was approved by and conducted in accordance with the Institutional Animal Care and Use Committee – Privately Owned Animal Protocol committee (IACUC-POAP #804586); informed owner consent was received for all procedures and conducted in accordance with the Privately Owned Animal Protocol committee.

A total of 112 presumably healthy ferrets were actively recruited; 57 ferrets were subsequently excluded for failure to meet the inclusion criteria. Ferrets determined to be clinically healthy based on history, physical examination performed by an exotic animal veterinarian, complete blood count, chemistry panel, urinalysis and follow-up owner contact were included in the study. All procedures were performed on the same day as diagnostic imaging. Owners were contacted regarding the health of their ferret following the study visit (mean 15 days, range 6 to 28 days) in an attempt to exclude those with occult illness at the time of imaging. Exclusion criteria included a history of either transient illness in the past six months or a long-term illness, administration of medications or the presence of any hormonal implant, any gross physical examination or clinicopathologic abnormality and manifestation of illness reported at any point in an individual's follow-up. Individuals were also excluded if they had gross radiographic or ultrasonographic abnormalities based on previously published guidelines for the adrenal glands in ferrets and based on our experience in ferrets and in other species (O'Brien *et al.* 1996, Neuwirth *et al.* 1997, Paul-Murphy *et al.* 1999, Kuijten *et al.* 2007, Garcia *et al.* 2011, Krautwald-Junghanns *et al.* 2011, Eshar *et al.* 2013). Ferrets were not excluded if a cutaneous mast cell tumour was the sole abnormality (n=3); cutaneous mast cell tumours are typically focal benign lesions in ferrets with visceral involvement and malignancy being rare (Orcutt & Tater 2012). Reasons for exclusion are summarised in Table S1 (Supporting Information).

Diagnostic imaging was performed and evaluated by a single board-certified radiologist. Three-view whole body radiographs (including the thorax, abdomen and pelvis) were obtained and included right lateral, left lateral, ventrodorsal projections (Canon LANMIX CXDI-50G detector; Sound-Eklin). Abdominal ultrasonography was performed using an 8 to 18 MHz linear transducer (GE Logiq S8 Vet, Sound-Eklin) with the exception of five ferrets at the initiation of the study which were imaged with a 6 to 15 MHz linear transducer (GE Medical LOGIQ 9 Ultrasound Imaging System; General Electric Medical Systems) due to equipment changes at our facility. Ferrets were scanned in dorsal recumbency. The ventral abdomen was shaved and warmed coupling gel was used. Ferrets were not fasted prior to imaging.

The spleen was radiographically identified using similar guidelines as in dogs and cats (Armbrust 2009). Whether the ventral extremity of the spleen was visible on the lateral radiographic projections along the ventral abdomen was recorded. On ultrasound, the splenic echotexture (homogeneous, mottled, nodular) and relative echogenicity (compared to the hepatic parenchyma and compared to the renal cortices) were recorded. With the spleen imaged in a longitudinal plane, parallel to the long axis, such that the splenic vein branches were evident along the mesenteric margin of the spleen, maximal thickness of the spleen was measured from the mesenteric margin to the anti-mesenteric margin (Fig 1A).

Radiographs were reviewed for distinguishable lymph nodes which were identified as small, round to oblong, soft-tissue opaque structures in the expected anatomic location of a lymph node and not associated with other visceral structures; these included sublumbar and caudal mesenteric nodes. The term "sublumbar lymph node" generally refers to lymph nodes from the iliosacral lymphocentre, including the medial iliac and internal iliac nodes, which may not be radiographically distinguishable from each other. The presence of a lymph node, number of nodes, maximal length and maximal thickness (perpendicular to the length measurement) were recorded.

Abdominal lymph nodes were ultrasonographically searched for and identified based on canine and feline anatomic references (Bezuidenhout 1993, d'Anjou 2008, Schreurs *et al.* 2008, Constantinescu & Schaller 2012, WAVA-ICVGAN 2012). Lymph nodes evaluated included the hepatic, pancreaticoduodenal, splenic, gastric, jejunal (mesenteric or cranial mesenteric), caudal mesenteric (left colic), colic, ileocolic (right colic), lumbar aortic (peri-aortic) and medial iliac lymph nodes (Fig 2). Localisation of the renal, internal iliac (hypogastric) and sacral nodes was attempted. The presence of a lymph node, number of nodes, maximal length, maximal thickness (perpendicular to the length measurement), echogenicity, identification of a hyperechoic hilus and cyst-like regions within lymph nodes were recorded. Echogenicity was classified as homogeneous, hyperechoic hilus with a hypoechoic rim, and heterogeneous (with or without a discernable hilus). The short-to-long axis ratio (S:L) was calculated for each lymph node. Lymph node shape was classified as rounded (S:L>0.5) or elongate (S:L$\leq$0.5), similar to prior studies (de Swarte *et al.* 2011, Beukers *et al.* 2013). Due to the U-shape or further serpentine shape of the large jejunal lymph nodes, length measurements for those lymph nodes were achieved by performing segmental linear measurements along the entire length of the node, then summing these values to achieve a total length (Fig 3). All measurements were performed in duplicate; measurements for each individual were averaged for analyses.

For the procedures ferrets were manually restrained or sedated. Manually restrained ferrets were given a liquid oil supplement (Ferre-Tone skin and coat supplement, 8 in 1 pet products) as a distraction and as a treat. Ferrets that resisted manual restraint or demonstrated escape behaviours during manual restraint were sedated. For sedation, 0.25 mg/kg midazolam (Sagent Pharmaceuticals) and 0.25 mg/kg butorphanol tartrate (Torbugesic; Fort Dodge Animal Health) were administered im (intramuscularly), and reversed respectively with im 0.01 mg/kg flumazenil (Hikma Farmaceutica) and 0.02 mg/kg naloxone (Hospira Inc) upon completion of imaging. All procedures were first discussed with owners and informed consent was obtained. This study was approved by the University of Pennsylvania Institutional Animal Care and Use Committee.

Data analysis

Statistical analyses employed were predominantly descriptive. The mean, standard deviation (SD) and 95% CI were calculated

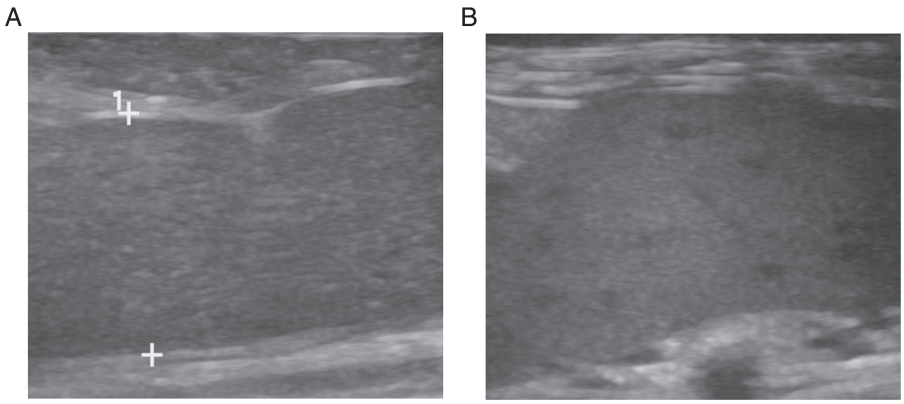

FIG 1. (A) Ultrasound images of the spleen in a ferret with a homogeneous splenic echotexture. Maximal splenic thickness measurements (callipers) were performed on images of the spleen parallel to its longitudinal axis and extended from the mesenteric margin to the anti-mesenteric margin. (B) Ultrasound image of the spleen in a ferret with a nodular echotexture; small, round, ill-defined, hypoechoic regions were identifiable throughout the splenic parenchyma

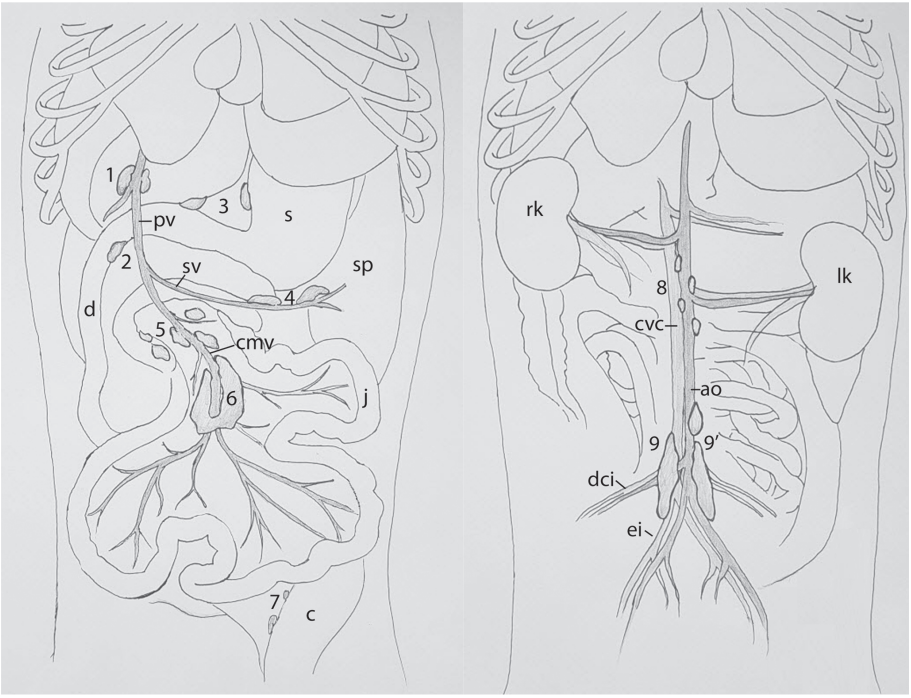

FIG 2. Schematic illustration of intra-abdominal lymph nodes and major vessels. Lymph nodes: 1 = hepatic, 2 = pancreaticoduodenal, 3 = gastric, 4 = splenic, 5 = cranial mesenteric group, 6 = jejunal, 7 = caudal mesenteric, 8 = lumbar aortic, 9 and 9′ = medial iliac. Vessels: ao = aorta, cmv = cranial mesenteric vein, cvc = caudal vena cava, dci = deep circumflex iliac vessels, ei = external iliac vessels, pv = portal vein, sv = splenic vein. Other landmarks: c = colon, d = duodenum, j = jejunoileum, s = stomach, sp = spleen, lk = left kidney, rk = right kidney. (From: Atlas of small animal ultrasonography by Penninck & d'Anjou (2008). Reproduced with permission of Blackwell Pub in the format Journal/magazine via Copyright Clearance Center. Minor changes were made to the original image)

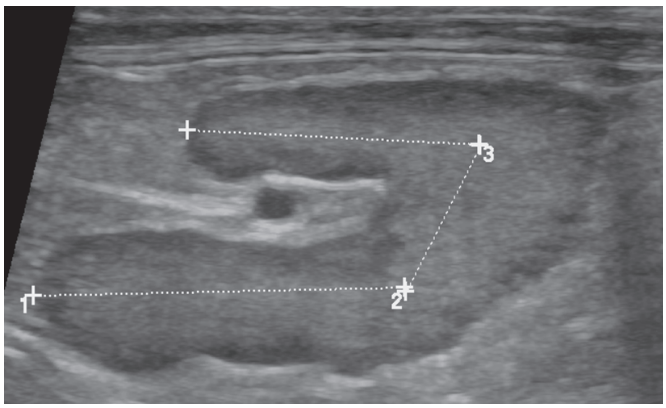

FIG 3. Ultrasound image of a jejunal lymph node. A single large jejunal lymph node was identified in all ferrets. The lymph node has a hyperechoic hilus and a hypoechoic rim. Because of the non-linear shape, length measurements were obtained by adding segmental linear measurements (callipers) along the long axes of the lymph node

for age, body weight and each organ measurement. Statistical analyses were performed using commercial statistics software (Stata/IC 12·1 for Windows).

RESULTS

Fifty-five ferrets were included in this study. Forty-two ferrets (76%) originated from commercial breeders and 13 (24%) from private breeders. Thirty-four ferrets were male (eight intact and 26 neutered males) and 21 were female (one intact and 20 neutered females). All sexually intact ferrets (9/55) were from private breeders. Of the neutered ferrets, 4 out of 20 neutered females were from private breeders and were neutered at a relatively later age (up to 1·8 years old) than those from commercial breeders (typically neutered before six weeks of age). With regards to body weight, intact males generally weighed more than neutered males, which generally weighed more than neutered females (Table 1). The single intact female in this study weighed more than the neutered females. Age at presentation ranged from four months to 4·2 years (mean ±SD: 1·9 ±1.0 years).

Sedatives were administered to 32 out of 55 ferrets (58%) to facilitate the procedures. There were no complications associated with sedation or any of the procedures.

Spleen

The spleen was radiographically identifiable in all ferrets. On ventrodorsal radiographs, the craniodorsal extremity was seen as a triangular soft-tissue opaque structure in the left side of the abdomen along the body wall, caudal to the stomach and craniolateral to the left kidney, and partly summating with the stomach and left kidney. The spleen then variably extended caudally or caudomedially as a broad curvilinear to crescentic soft-tissue structure. On lateral radiographic projections, the craniodorsal extremity of the spleen could be seen as a triangular soft-tissue opaque structure in the craniodorsal abdomen, caudal to the gastric fundus. The spleen could then sometimes be seen extending caudoventrally in the mid-abdomen as a broad, curvilinear

soft-tissue opaque structure summating with the intestines. On lateral radiographic projections, the spleen could be seen along the ventral abdomen in 21 out of 55 (38%) ferrets; in 4 out of 21 (19%) this was seen only on the right lateral projection and in 5 out of 21 (24%) only on the left lateral projection. The spleen was more frequently visible along the ventral abdomen in male ferrets (17 out of 21; 81% males) than female ferrets (4 out of 21; 19% females) and in sedated (16 out of 21; 76%) than non-sedated (5 out of 21; 24%) ferrets.

On ultrasound, the spleen was identified in the left lateral abdomen. The spleen was hyperechoic relative to the liver (55 out of 55). The spleen was mildly hyperechoic to the renal cortices in 28 out of 55 (51%) ferrets, isoechoic in 15 out of 55 (27%) and mildly hypoechoic in 12 out of 55 (22%). It had a homogeneous echotexture in 38 out of 55 (69%), a mildly mottled echotexture in 12 out of 55 (22%), and had ill-defined, round, hypoechoic nodules in 5 out of 55 (9%) (Fig 1). The three ferrets with presumptively incidental cutaneous mast cell tumours all had a homogeneous splenic echotexture.

With ultrasound the mean splenic thickness measurement was 11·80 ±0·34 mm (95% CI: 11·12 to 12·49 mm; range 8·16 to 17·70 mm). The mean thickness was a little more in ferrets in which the spleen was radiographically detected along the ventral abdomen (12·75 ±0·63 mm) compared to those in which it was not (11·24 ±0·37 mm).

Abdominal lymph nodes

Lymph nodes were radiographically discernible in 28 out of 55 (51%) ferrets. The radiographic frequency of lymph node detection and measurements are summarised in Table 2.

Caudal mesenteric lymph nodes were seen on lateral abdominal radiographs in 24 out of 55 (44%) ferrets. Caudal mesenteric lymph nodes were identified as well-defined, oblong, soft-tissue opaque structures in the caudal abdomen dorsal and immediately adjacent to the descending colon at the level of L5 to L6 (Fig 4).

Table 1. Body weight distribution between female and male ferrets. Body weight was significantly associated with sex and neuter status (p<0.0001)

	N	Body weight (kg)	
	(Frequency)	Mean ±SD	Range
Overall	55 (100%)	1·10 ±0·30	0·60 to 1·84
Female, neutered	20 (36%)	0·79 ±0·11	0·60 to 0·95
Female, intact	1 (2%)	1·6	
Male, neutered	26 (47%)	1·18 ±0·15	0·95 to 1·54
Male, intact	8 (15%)	1·58 ±0·16	1·41 to 1·84

N Number of ferrets, SD Standard deviation

One caudal mesenteric lymph node was distinguishable in 21 ferrets and two nodes were distinguishable in three ferrets.

Sublumbar lymph nodes were seen on lateral abdominal radiographs in 6 out of 55 (11%) ferrets. Sublumbar lymph nodes were identified as well-defined, oblong, soft-tissue opaque structures in the caudal retroperitoneal space ventral to L5 and L6 (Fig 5). One sublumbar lymph node was distinguishable in five ferrets and two nodes were distinguishable in one ferret. As the medial iliac lymph node was the only iliosacral lymphocentre node that was ultrasonographically identified, the sublumbar lymph nodes that were radiographically detected presumably represent medial iliac lymph nodes.

Lymph nodes were found with ultrasound in the expected locations and corresponding anatomic landmarks (Fig 2) as previously reported for dogs and cats (Bezuidenhout 1993, d'Anjou 2008, Schreurs *et al.* 2008, Constantinescu & Schaller 2012). Detected lymph nodes included jejunal, pancreaticoduodenal, hepatic, caudal mesenteric, splenic, gastric, medial iliac and lumbar aortic lymph nodes. Small lymph nodes were also seen in the mid-abdomen and were difficult to differentiate as ileocolic lymph nodes, colic lymph nodes or additional smaller jejunal lymph nodes. These were often seen in close proximity and slightly cranial to the single large jejunal lymph node. Because these small nodes were not distinguishable as specific lymph nodes, these were grouped and termed cranial mesenteric lymph nodes.

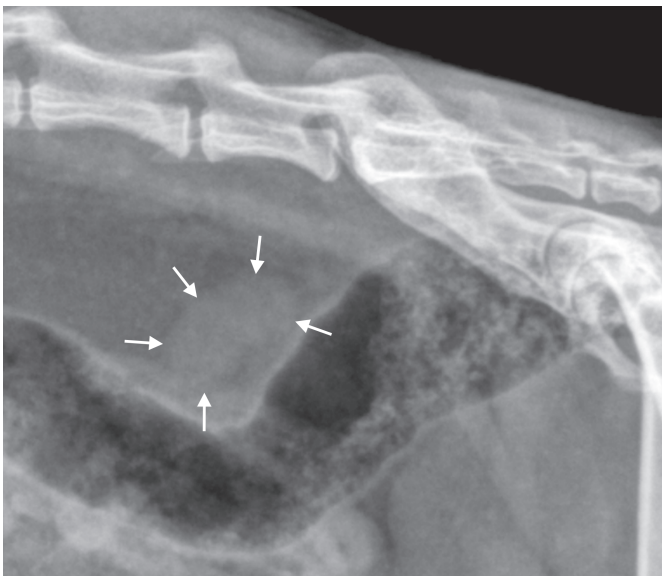

FIG 4. Lateral radiograph of the caudal abdomen in which a caudal mesenteric lymph node (arrows) is appreciable. Caudal mesenteric lymph nodes were identified dorsal and adjacent to the descending colon

Table 2. Radiographic frequency of abdominal lymph node detection on lateral radiographs, number of lymph nodes detected and measurements

	N	n	Thickness (mm)			Length (mm)		
	(Frequency)	(Mode)	Mean ±SD	95% CI	Range	Mean ±SD	95% CI	Range
Caudal mesenteric	24 (43·6%)	1 to 2 (1)	4·8 ±1·9	4·0 to 5·6	1·7 to 8·8	9·2 ±3·5	7·7 to 10·6	2·6 to 16·3
Sublumbar	6 (10·9%)	1 to 2 (1)	4·0 ±1·7	2·2 to 5·7	1·8 to 5·9	9·5 ±3·0	6·2 to 12·7	5·8 to 13·8

N Number of ferrets in which the lymph node was detected, n Number of lymph nodes detected in individual ferrets, SD Standard deviation, CI Confidence interval

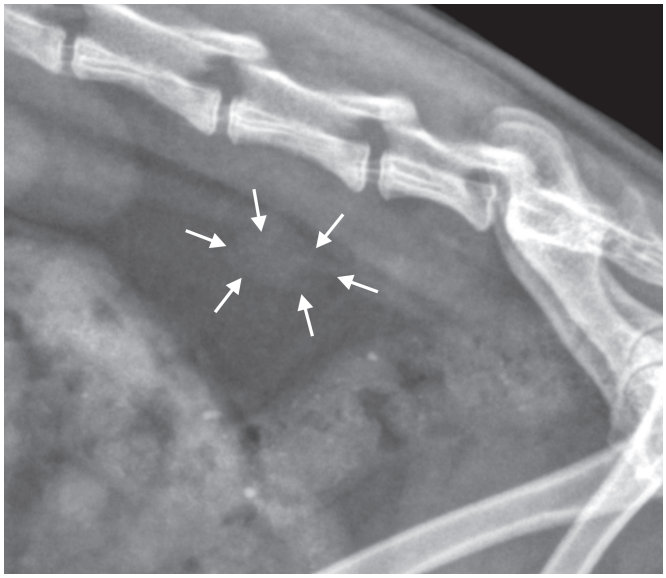

FIG 5. Lateral radiograph of the caudal abdomen in which a sublumbar lymph node (arrows) is appreciable in the retroperitoneal space ventral to L5

A summary of the ultrasonographic features and measurements for abdominal lymph nodes are provided in Tables 3 and 4, respectively. Lymph node thickness measurements are also graphically depicted in Fig 6. An average and SD of 9 ±2 lymph nodes (mode 10 lymph nodes; range 5 to 14 lymph nodes) were identified in each ferret. A single large jejunal lymph node was identified in all ferrets. All lymph nodes were oblong, with the exception of the single large jejunal lymph node which was U-shaped or serpentine (Fig 3). Most lymph nodes were hypoechoic relative to the surrounding mesenteric fat with a more echogenic central hilus (Fig 3). Homogeneous lymph nodes were either hypoechoic or mildly hyperechoic. Heterogeneous lymph nodes were mildly heterogeneous and mildly hyperechoic. Several of the heterogeneous lymph nodes were predominantly hyperechoic with discontinuous hypoechoic marginal regions, not forming a complete hypoechoic rim. Anechoic cyst-like regions (Fig 7) were identified in 31 out of a total of 492 lymph nodes (6.3%) evaluated, and were most frequently detected in the pancreaticoduodenal lymph nodes (10 out of 31; 32·3% of cystic lymph nodes) followed by the hepatic lymph nodes (5 out of 31; 16·1% of cystic lymph nodes). Lymph nodes with cyst-like changes were present in 14 out of 55 (25·5%) ferrets. Cyst-like changes were present in one lymph node in seven ferrets, two lymph nodes in two ferrets, three lymph nodes in four ferrets and eight lymph nodes in one ferret. The mean age of ferrets with cyst-like regions was 2·79 ±0·85 years (range: 1·5 to 4·2 years), compared to the mean age of ferrets without detected cyst-like regions, 1·53 ±0·85 years (range: 4 months to 3·7 years).

DISCUSSION

The results presented in this study provide the most comprehensive evaluation of the spleen and abdominal lymph nodes with radiographs and ultrasound in clinically healthy ferrets to date.

Table 3. Ultrasonographic features of abdominal lymph nodes in ferrets. Lymph node shape was recorded as round or elongate based on the short-to-long axis ratio (S:L); the mode shape is provided in the table. Lymph nodes with a S:L greater than 0.5 were characterised as round, while those with an S:L less than or equal to 0.5 were characterised as elongate. The number of ferrets in which cyst-like changes were detected or in which a hyperechoic hilus was appreciable is also reported. Lymph node echogenicity was recorded as either homogeneous (either hypoechoic or mildly hyperechoic), hilar (having a hypoechoic rim and hyperechoic hilus) or heterogeneous (mildly heterogeneous and hyperechoic with or without a discernable hilus)

	N (frequency)	Shape, mode (S:L mean ±SD)	Cyst-like changes	Hilus identified	Echogenicity		
					Homogeneous	Hilar	Heterogeneous
Visceral nodes							
Jejunal (single large)	55 (100%)	Elongate* (0·21 ±0·07)	1 (1·8%)	55 (100%)	0	54 (98·2%)	1 (1·8%)
Pancreaticoduodenal	53 (96·4%)	Round (0·53 ±0·14)	10 (18·9%)	39 (73·6%)	7 (13·2%)	35 (66·0%)	11 (20·8%)
Hepatic	52 (94·5%)	Elongate (0·37 ±0·11)	5 (9·6%)	40 (76·9%)	10 (19·2%)	31 (59·6%)	11 (21·2%)
Cranial mesenteric (group)	47 (85·5%)	Round (0·52 ±0·20)	3 (6·4%)	40 (85·1%)	4 (8·5%)	39 (83·0%)	4 (8·5%)
Caudal mesenteric	46 (83·6%)	Elongate (0·50 ±0·15)	2 (4·4%)	35 (76·1%)	6 (13·0%)	32 (69·6%)	8 (17·4%)
Splenic	38 (69·1%)	Round (0·55 ±0·20)	2 (5·3%)	20 (52·6%)	11 (29·0%)	20 (52·6%)	7 (18·4%)
Gastric	33 (60·0%)	Elongate (0·49 ±0·17)	2 (6·1%)	28 (84·9%)	4 (12·1%)	28 (84·9%)	1 (3·0%)
Parietal nodes							
Left medial iliac	44 (80·0%)	Elongate (0·21 ±0·09)	0	22 (50%)	17 (38·6%)	20 (45·5%)	7 (15·9%)
Right medial iliac	39 (70·9%)	Elongate (0·20 ±0·07)	0	22 (57·9%)	12 (31·6%)	21 (55·3%)	5 (13·2%)
Lumbar aortic	7 (12·7%)	Elongate (0·39 ±0·13)	1 (11·1%)	5 (71·4%)	1 (14·3%)	4 (57·1%)	2 (28·6%)

N Number of ferrets in which the lymph node was detected, S:L Short-to-long axis ratio, SD Standard deviation
*The single large jejunal lymph node was elongate and serpentine

Table 4. Ultrasonographic frequency of abdominal lymph node detection, number of lymph nodes detected and measurements

	N (Frequency)	n (Mode)	Thickness (mm) Mean±SD	95% CI	Range	Length (mm) Mean±SD	95% CI	Range
Visceral nodes								
Jejunal (single large)	55 (100%)	1	5·28±1·66	4·84 to 5·73	0·39 to 10·46	26·34±7·50	24·31 to 28·37	12·08 to 48·30
Pancreaticoduodenal	53 (96·4%)	1 to 2 (1)	3·30±1·06	3·01 to 3·59	1·42 to 6·60	6·38±1·82	5·88 to 6·89	3·10 to 12·98
Hepatic	52 (94·5%)	1 to 2 (1)	3·22±1·12	2·91 to 3·54	1·10 to 8·10	9·14±3·35	8·21 to 10·08	3·12 to 21·10
Cranial mesenteric (group)	47 (85·5%)	1 to 3 (1)	3·38±0·99	3·09 to 3·37	0·90 to 6·90	7·61±3·39	6·61 to 8·60	2·13 to 15·39
Caudal mesenteric	46 (83·6%)	1 to 3 (1)	2·76±0·76	2·53 to 2·98	0·98 to 7·62	5·91±2·12	5·28 to 6·54	1·86 to 15·06
Splenic	38 (69·1%)	1 to 3 (2)	2·71±0·94	2·40 to 3·02	0·80 to 6·93	5·62±2·95	4·65 to 6·57	1·80 to 16·80
Gastric	33 (60·0%)	1 to 2 (1)	3·14±0·93	2·81 to 3·47	1·42 to 5·37	6·77±2·09	6·03 to 7·51	1·72 to 11·40
Parietal nodes								
Left medial iliac	44 (80·0%)	1 to 2 (1)	1·98±0·73	1·75 to 2·20	0·80 to 4·30	10·03±3·61	8·94 to 11·13	1·04 to 23·02
Right medial iliac	39 (70·9%)	1	1·87±0·53	1·70 to 2·05	0·92 to 3·29	9·72±3·04	8·72 to 10·72	5·14 to 16·99
Lumbar aortic	7 (12·7%)	1 to 2 (1)	2·36±1·47	1·00 to 3·72	1·06 to 3·34	6·23±2·68	3·76 to 8·71	2·21 to 8·81

N Number of ferrets in which the lymph node was detected, n Number of lymph nodes detected in individual ferrets, SD Standard deviation, CI Confidence interval

The spleen was radiographically detectable in all ferrets, and had a similar appearance to that previously described in dogs and cats (Armbrust 2009). In cats, the spleen is considered enlarged if the body or ventral extremity is visible along the ventral abdomen on lateral radiographs. Aside from this guideline, radiographic assessment of splenic size is subjective in cats and dogs (Armbrust 2009). The spleen was radiographically visible along the ventral abdomen in 38% of the clinically healthy ferrets in this study and therefore cannot be used as a general guideline to determine if the spleen is enlarged. Additionally, as the body and ventral extremity of the spleen are mobile, splenic position within the abdomen may affect the radiographic appearance. Specific radiographic guidelines to determine enlargement were not determined in this study; subjective radiographic assessment of the ferret spleen is therefore warranted in ferrets.

Gross splenic measurements have been previously reported as 5·10 cm length×1·80 cm width.0·80 cm thick (Evans & An 2014). The thickness measurements obtained in this study using ultrasound were all greater than previously reported with the smallest thickness measurement in this study being 8·16 mm. These discrepancies in measurements may result from differences between in vivo *versus* post-mortem sampling. Signalment and body weight differences may also contribute but this information was not available for the ferrets in which the gross measurements were derived.

On ultrasound, the spleen was hyperechoic to the liver. The relative echogenicity of the spleen compared to the renal cortices was variable, but most frequently the spleen was hyperechoic to the renal cortex. In cats fat may be deposited in the renal cortex and results in increased cortical echogenicity; this is associated with sex hormones in cats and is not associated with body weight (Yeager & Anderson 1989, Maxie 1993). It is unknown whether renal cortical fat deposition also occurs in ferrets.

The spleen had a homogeneous echotexture in 69% of ferrets. A mildly mottled echotexture or ill-defined small hypoechoic regions were seen in 31% of ferrets. Causes for a non-homogeneous echogenicity may include potentially incidental etiologies such as nodular hyperplasia or extramedullary hematopoiesis, which commonly occurs in adult ferrets, although other subclinical pathologies, such as lymphoma or splenitis, cannot be excluded. Ferrets with a non-homogeneous splenic echogenicity were not excluded as the ferrets remained clinically healthy throughout the study and follow-up period (Levaditi *et al.* 1959, Mayer *et al.* 2014).

This is the first study to describe radiographic appearance of presumed normal lymph nodes in ferrets and those detected included the caudal mesenteric and sublumbar lymph nodes. At least one lymph node was radiographically discernible in 51% of ferrets in this study. Radiographic lymph node measurements were generally greater than ultrasound measurements. The differences in measurements between imaging modalities is likely due to magnification on radiographs. Silhouetting or superimposition of adjacent lymph nodes may also contribute to larger measurements on radiographs. Additionally, measurements may be affected by patient positioning. The provided measurements are intended as a descriptor for lymph node dimensions. The poten-

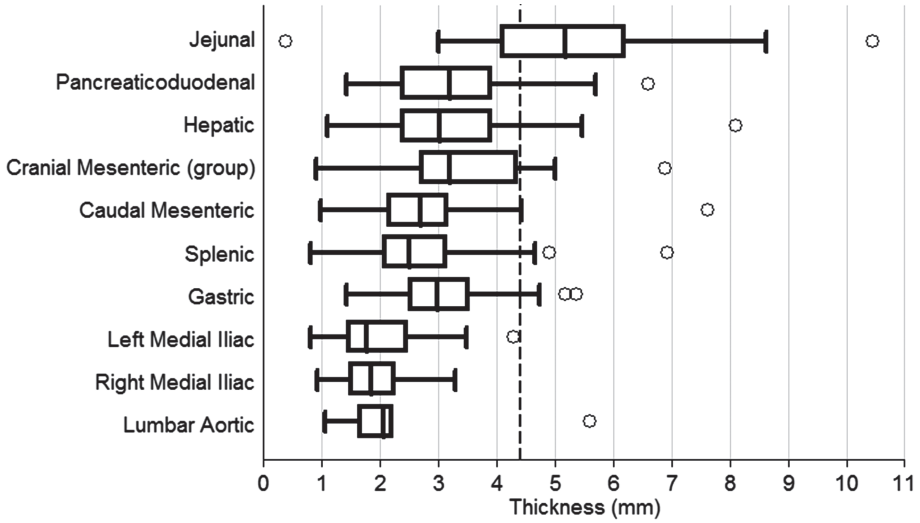

FIG 6. Box plot of ultrasonographic lymph node thickness measurements. Boxes represent the interquartile range (25th to 75th). The vertical bar within the box is the median. The T-bars represent the range. Circles represent outliers. With the exception of the single large jejunal lymph node, the mean values plus one SD were less than 4.4 mm (dashed reference line)

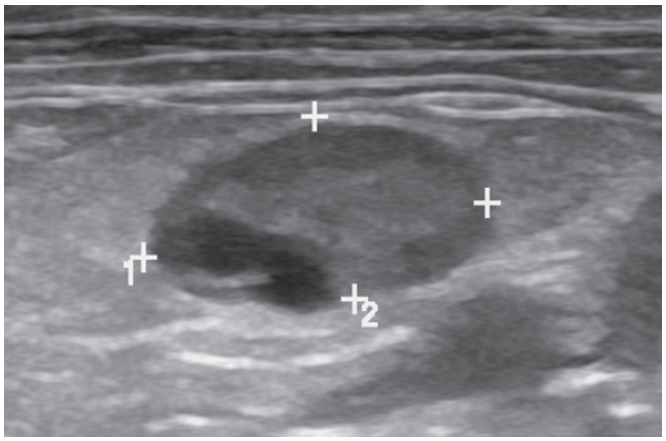

FIG 7. Anechoic cyst-like changes in a gastric lymph node. The lymph node has a hyperechoic hilus and a hypoechoic rim and contains a lobular, anechoic cyst-like region

tial clinical utility for radiographic lymph node measurements is questionable as the use of measurements for radiographic image interpretation has not been found to be more accurate than subjective image interpretation (Lamb & Nelson 2015).

Multiple lymph node groups were detectable with ultrasound. Similar to previous studies, a single large jejunal lymph node (also known as mesenteric or cranial mesenteric lymph node) was detected in all ferrets (Paul-Murphy *et al.* 1999, Garcia *et al.* 2011). The detection frequencies of the hepatic, pancreaticoduodenal, splenic and gastric lymph nodes were much higher than previously reported (Garcia *et al.* 2011).

Because of the overall small patient size, detection and differentiation of lymph nodes can be difficult. With the small size of ferrets, structures in the abdomen are relatively close together; additionally, compression of the abdomen and abdominal viscera which occur during ultrasonography may further compound this. Small lymph nodes in the mid-abdomen just cranial to the single large jejunal lymph node were difficult to differentiate as ileocolic lymph nodes, additional colic lymph nodes (possibly middle colic lymph nodes), additional smaller jejunal lymph nodes or a combination thereof. Some of these nodes were suspected to be ileocolic lymph nodes, although the ileocolic junction is not readily identifiable in ferrets, which complicates identification of lymph nodes as ileocolic lymph nodes (Evans & An 2014). As the specific lymph node location could not be determined for these small lymph nodes and they likely belonged to the cranial mesenteric lymphocentre, they were termed cranial mesenteric lymph nodes. In carnivores, the cranial mesenteric lymphocentre is comprised of the ileocolic, colic and jejunal lymph nodes (Bezuidenhout 1993, Constantinescu & Schaller 2012). The clinical relevance and importance of separating these small mid-abdominal lymph nodes into ileocolic, colic and jejunal lymph nodes is not known.

Based on the results of this study, the jejunal, pancreaticoduodenal, hepatic and caudal mesenteric lymph nodes can be routinely detected with ultrasound in most ferrets. The pancreaticoduodenal and hepatic lymph nodes were detected in 96·4% (53 out of 55) and 94·5% (52 out of 55) of ferrets, respectively. It is possible that these lymph nodes were not detected in those two and three ferrets, respectively, due to patient disposition and human error. For the caudal mesenteric lymph nodes, 8 out of 9 individuals in which the caudal mesenteric lymph nodes were not ultrasonographically detected were imaged at the initiation of this study. It is suspected that the caudal mesenteric lymph nodes were not detected, as opposed to not present, in those individuals, and after a steep learning curve these lymph nodes were routinely identified. The medial iliac lymph nodes were detected at a relatively high frequency as well; however, their small size (specifically thickness) made them more difficult to detect than others. With the exception of the single large jejunal lymph node, the mean value plus one SD for thickness measurements were all less than 4·4 mm and the upper ranges of the 95% CI were less or equal to than 3·72 mm.

Although previous studies using ultrasound reported detection of a single large jejunal lymph node, an anatomical reference

for ferrets mentions both a left and right lymph node (Paul-Murphy *et al*. 1999, Garcia *et al*. 2011, Evans & An 2014). In this study, a single large jejunal lymph node was identified with ultrasound in all ferrets; additional smaller lymph nodes in the vicinity of the jejunal lymph node may have represented smaller jejunal lymph nodes, ileocolic lymph nodes and/or colic lymph nodes. The mean jejunal lymph node thickness in this study (5·28 ±1·66 mm) was similar to the previously reported mean of 5·3 mm by Garcia *et al*. (2011), but was less than the previously reported mean of 7.6 mm in the study by Paul-Murphy *et al*. (1999). In the study by Paul-Murphy *et al*. (1999), cytology was performed on a portion of the jejunal lymph nodes and demonstrated relatively high numbers of eosinophils in 55% of sampled nodes which may represent a normal variant in ferrets or may have represented occult disease (Paul-Murphy *et al*. 1999). Cytology was not performed in this study or in that by Garcia *et al*. (2011). The mean jejunal lymph node length measurement (26·34 ±7·50 mm) was greater than the previously reported mean values (12·6 ±2·6 and 5·3 ±1·39 mm) (Paul-Murphy *et al*. 1999, Garcia *et al*. 2011); this is suspected to be due to differences in methodology. Because the jejunal lymph node was serpentine, segmented linear measurements were summed to determine the total length. Although the specific technique was not described in the previous studies, presumably a single linear measurement was previously performed along the long axis of the largest part of the lymph node. This presumed difference in technique would account for the length measurements in this study being greater than previously reported. In general, lymph node thickness measurements and short-to-long axis ratios may have more clinical utility than evaluation of length measurements alone. When lymph nodes enlarge, they tend to become more rounded, having a greater short-to-long axis ratio; this change is attributed to a greater increase in thickness measurements compared to length measurements (de Swarte *et al*. 2011). In humans and dogs, evaluation of the short-to-long axis ratio may assist in differentiating benign *versus* malignant neoplastic lymphadenopathies; a greater short-to-long axis ratio is associated with neoplastic lymphadenopathy while a lesser short-to-long axis ratio is associated with normal and reactive or inflammatory lymphadenopathies (Nyman *et al*. 2004, de Swarte *et al*. 2011).

Cyst-like changes were identified in 6·3% (31 out of 492) of all lymph nodes evaluated in this study and were more frequently identified in older ferrets. This finding is of unknown clinical significance, particularly since cyst-like changes were recognised in 25·5% (14 out of 55) of the clinically healthy ferrets of this study. Cyst-like changes are suspected to represent lymphatic sinus ectasia (lymphangectasia, lymphatic cysts, cystic lymphatic ectasia or sinus dilation). Hyperplastic lymph nodes are common in older ferrets secondary to underlying gastrointestinal inflammation (Antinoff & Williams 2012). Overt gastrointestinal abnormalities were not ultrasonographically detected in ferrets included for data analysis, and ferrets with clinical signs referable to the gastrointestinal tract were excluded; however, lymph node hyperplasia secondary to subclinical gastrointestinal or non-gastrointestinal pathology cannot be excluded. In rats and mice, lymphatic sinus ectasia is associated with lymphoid atrophy and can be seen in ageing animals (Sainte-Marie *et al*. 1997, Elmore 2006). In humans, cyst-like areas in lymph nodes can be seen with metastatic neoplasia, particularly secondary to necrosis. Cystic necrosis results in an anechoic area within the lymph node and is commonly found in metastatic lymph nodes in humans. Coagulative nodal necrosis is uncommonly seen, results in an echogenic area and can be seen in malignant and inflammatory lymph nodes (Ahuja & Ying 2003). Nodules comprised of neoplastic cells may also have a pseudocystic appearance on ultrasound (Ahuja & Ying 2003). Less frequently nodal metastasis may produce a true cyst with an epithelial lining (Verma *et al*. 1994). Further studies with histopathologic evaluation of cystic lymph nodes and to evaluate the clinical significance of this change are warranted.

Because of the small patient size, adrenal glands can be mistaken for lymph nodes and vice versa. The hepatic lymph nodes may be mistaken for the right adrenal gland, for example. The portal vein and caudal vena cava can be seen relatively close together in the cranial abdomen of ferrets. Additionally the caudal vena cava is easily compressed from pressure of the ultrasound transducer during ultrasonography. Although both the portal vein and caudal vena cava may be seen adjacent to the hepatic lymph nodes, the hepatic lymph nodes are more closely associated with the portal vein, while the right adrenal gland is in close apposition to the caudal vena cava. Careful evaluation of lymph nodes relative to their anatomic landmarks, which are crucial for differentiating lymph nodes from each other and from the adrenal glands and which are in close vicinity to other landmarks, is warranted.

The major limitations of the study included external validity (generalisability), selection bias, misclassification bias and human error (reliability and internal consistency). The ferrets in this study may not be representative of the general population; most ferrets in this study, in common with most in the USA, originated from a single large commercial breeder. Additionally there were very few sexually intact ferrets. The generalisability of the findings in this study to ferrets from geographic locations outside of the USA is difficult to judge. Another limitation is that there was no gold standard to confirm a disease-free status. Organ sampling was not within the scope of this study. As an imperfect surrogate, we used the individual's history, physical exam, blood work, urinalysis and follow-up owner contact. Diagnostic imaging findings did result in some patients being excluded, who may bias the data and result in exclusion of normal variants; however, based on our experiences with ultrasound in ferrets and in other species, those individuals were considered very likely to be abnormal. The included ferrets were clinically healthy throughout the study and follow-up interim. Inter-observer and intra-observer differences were not evaluated.

In summary, the information provided in this study may act as a baseline for evaluation of the spleen and lymph nodes in ferrets. On radiographs the spleen was visible in all ferrets, and the sublumbar or caudal mesenteric lymph nodes were discernible in 51% of ferrets. With ultrasound the spleen was hyperechoic to the liver and most often had a homogeneous

or mildly mottled echotexture; additionally, multiple lymph nodes were identified. The jejunal, pancreaticoduodenal, hepatic and caudal mesenteric lymph nodes can be routinely detected with ultrasound. The jejunal lymph node was seen in all ferrets and had a mean thickness of 5·28 ±1·66 mm. The mean thickness measurements plus one SD for all other lymph nodes were less than 4.4 mm. Additional studies evaluating the clinical utility and predictive validity of the provided measurements are warranted.

Acknowledgements

Funding was provided by an institutional grant from the University of Pennsylvania and a donation from Abaxis. The authors would like to acknowledge and thank Bruce Williams for consultation on histopathology; Thomas Tyson for medical illustration; Mary Baldwin, Alisa Rassin and Max Emanuel for technical assistance and Scales and Tails Rescue for assistance with recruitment.

Conflict of interest

No conflicts of interest have been declared.

References

d'Anjou, M.-A. (2008) Abdominal cavity, lymph nodes, and great vessels. In: Atlas of Small Animal Ultrasonography. Eds D. Penninck and M.-A. d'Anjou. Blackwell Publishing, Ames, IA, USA. pp 445-463

Ahuja, A. & Ying, M. (2003) Sonography of neck lymph nodes. Part II: abnormal lymph nodes. *Clinical Radiology* **58**, 359-366

Antinoff, N. & Williams, B. H. (2012) Neoplasia. In: Ferrets, Rabbits, and Rodents. 3rd edn. Eds K. E. Carpenter and J. W. Quesenberry. W.B. Saunders, Saint Louis, MO, USA. pp 103-121

Armbrust, L. (2009) The spleen. In: BSAVA Manual of Canine and Feline Abdominal Imaging. Eds R. O'Brien and F. Barr. British Small Animal Veterinary Association, Gloucester, UK. pp 167-176

Beukers, M., Grosso, F. V. & Voorhout, G. (2013) Computed tomographic characteristics of presumed normal canine abdominal lymph nodes. *Veterinary Radiology & Ultrasound* **54**, 610-617

Bezuidenhout, A. (1993) The lymphatic system. In: Miller's Anatomy of the Dog. 3rd edn. Ed H. E. Evans. WB Saunders Company, Philadelphia, PA, USA. pp 717-757

Constantinescu, G. M. & Schaller, O. (2012) Illustrated Veterinary Anatomical Nomenclature. 3rd edn. Enke Verlag, Stuttgart, Germany vi, 614 p

Dominguez, E., Novellas, R., Moya, A., Espada, Y. & Martorell, J. (2011) Abdominal radiographic and ultrasonographic findings in ferrets (Mustela putorius furo) with systemic coronavirus infection. *The Veterinary Record* **169**, 231

Elmore, S. A. (2006) Histopathology of the lymph nodes. *Toxicologic Pathology* **34**, 425-454

Eshar, D., Mayer, J., Parry, N. M., Williams-Fritze, M. J. & Bradway, D. S. (2010) Disseminated, histologically confirmed Cryptococcus spp infection in a domestic ferret. *Journal of the American Veterinary Medical Association* **236**, 770-774

Eshar, D., Briscoe, J. A. & Mai, W. (2013) Radiographic kidney measurements in North American pet ferrets (Mustela furo). *Journal of Small Animal Practice* **54**, 15-19

Evans, H. & An, N. Q. (2014) Anatomy of the ferret. In: Biology and Diseases of the Ferret. 3rd edn. Eds J. G. Fox and R. P. Marini. John Wiley & Sons, Inc., Ames, IA, USA. pp 23-67

Ferguson, D. C. (1985) Idiopathic hypersplenism in a ferret. *Journal of the American Veterinary Medical Association* **186**, 693-695

Fox, J. G. (2014) Normal clinical and biological parameters. In: Biology and Diseases of the Ferret. 3rd edn. Eds J. G. Fox and R. P. Marini. John Wiley & Sons, Inc., Ames, IA, USA. pp 157-185

Garcia, D. A. A., da Silva, L. C. S., Lange, R. R. & Froes, T. R. (2011) Anatomia ultrassonográfica dos linfonodos abdominais de furões europeus hígidos [Ultrasonographic anatomy of abdominal lymph nodes in healthy European ferrets]. *Pesquisa Veterinária Brasileira [Brazilian Journal of Veterinary Research]* **31**, 1129-1132

Hulley, S. (2007) Appendix 6d: sample size for a descriptive study of a continuous variable. In: Designing Clinical Research. Lippincott Williams & Wilkins, Philadelphia, PA, USA. p 90

Krautwald-Junghanns, M.-E., Pees, M., Reese, S. & Tully, T. (2011) Diagnostic Imaging of Exotic Pets. Schlutersche, Hannover, Germany

Kuijten, A. M., Schoemaker, N. J. & Voorhout, G. (2007) Ultrasonographic visualization of the adrenal glands of healthy ferrets and ferrets with hyperadrenocorticism. *Journal of the American Animal Hospital Association* **43**, 78-84

Lamb, C. R. & Nelson, J. R. (2015) Diagnostic accuracy of tests based on radiologic measurements of dogs and cats: a systematic review. *Veterinary Radiology & Ultrasound* **56**, 231-244

Levaditi, J., Chandli, A. & Vallée, A. (1959) Activité hémopoïétique de la rate du Vison (Mustela lutreola) et du Furet (Mustela putrius furo) [Hemopoietic activity of the mink and ferret spleen]. *Comptes Rendus des Seances de la Societe de Biologie et de ses Filiales* **153**, 222-225

Lindemann, D. M., Eshar, D., Schumacher, L. L., Almes, K. M. & Rankin, A. J. (2016) Pyogranulomatous panophthalmitis with systemic coronavirus disease in a domestic ferret (Mustela putorius furo). *Veterinary Ophthalmology* **19**, 167-171

Maxie, M. (1993) The urinary system. In: Pathology of Domestic Animals. 4th edn. Eds K. V. F. Jubb, P. C. Kennedy and N. Palmer. Academic Press Inc, San Diego, CA, USA. pp 447-454

Mayer, J., Erdman, S. E. & Fox, J. G. (2014) Diseases of the hematopoietic system. In: Biology and Diseases of the Ferret. 3rd edn. Eds J. G. Fox and R. P. Marini. John Wiley & Sons, Inc., Ames, IA, USA. pp 311-334

Morrisey, J. K. & Kraus, M. S. (2012) Cardiovascular and other diseases. In: Ferrets, Rabbits, and Rodents. 3rd edn. Eds K. E. Carpenter and J. W. Quesenberry. W.B. Saunders, Saint Louis, CA. USA. pp 62-77

Nakata, M., Miwa, Y., Tsuboi, M. & Uchida, K. (2014) Mycobacteriosis in a domestic ferret (Mustela putorius furo). *Journal of Veterinary Medical Science* **76**, 705-709

Neuwirth, L., Collins, B., Calderwood-Mays, M. & Tran, T. (1997) Adrenal ultrasonography correlated with histopathology in ferrets. *Veterinary Radiology & Ultrasound* **38**, 69-74

Nyman, H. T., Kristensen, A. T., Flagstad, A. & McEvoy, F. J. (2004) A review of the sonographic assessment of tumor metastases in liver and superficial lymph nodes. *Veterinary Radiology & Ultrasound* **45**, 438-448

O'Brien, R. T., Paul-Murphy, J. & Dubielzig, R. R. (1996) Ultrasonography of adrenal glands in normal ferrets. *Veterinary Radiology & Ultrasound* **37**, 445-448

Orcutt, C. & Tater, K. (2012) Dermatologic diseases. In: Ferrets, Rabbits, and Rodents. 3rd edn. Eds K. E. Carpenter and J. W. Quesenberry. W.B. Saunders, Saint Louis, MO, USA. pp 122-131

Paul-Murphy, J., O'Brien, R. T., Spaeth, A., Sullivan, L. & Dubielzig, R. R. (1999) Ultrasonography and fine needle aspirate cytology of the mesenteric lymph node in normal domestic ferrets (Mustela putorius furo). *Veterinary Radiology & Ultrasound* **40**, 308-310

Pollock, C. (2012) Mycobacterial infection in the ferret. *The Veterinary Clinics of North America. Exotic Animal Practice* **15**, 121-129, vii

Sainte-Marie, G., Peng, F. & Guay, G. (1997) Ectasias of the subcapsular sinus in lymph nodes of athymic and euthymic rats: a relation to immunodeficiency. *Histology and Histopathology* **12**, 637-643

Schreurs, E., Vermote, K., Barberet, V., Daminet, S., Rudorf, H. & Saunders, J. H. (2008) Ultrasonographic anatomy of abdominal lymph nodes in the normal cat. *Veterinary Radiology & Ultrasound* **49**, 68-72

Schwarz, L. A., Solano, M., Manning, A., Marini, R. P. & Fox, J. G. (2003) The normal upper gastrointestinal examination in the ferret. *Veterinary Radiology & Ultrasound* **44**, 165-172

de Swarte, M., Alexander, K., Rannou, B., D'Anjou, M.-A., Blond, L. & Beauchamp, G. (2011) Comparison of sonographic features of benign and neoplastic deep lymph nodes in dogs. *Veterinary Radiology & Ultrasound* **52**, 451-456

Verma, K., Mandal, S. & Kapila, K. (1994) Cystic change in lymph nodes with metastatic squamous cell carcinoma. *Acta Cytologica* **39**, 478-480

WAVA-ICVGAN (2012) Nomina Anatomica Veterinaria, 5th ed (revised). ICVGAN Editorial Committee, Columbia, MO, USA

Yeager, A. & Anderson, W. (1989) Study of association between histologic features and echogenicity of architecturally normal cat kidneys. *American Journal of Veterinary Research* **50**, 860-863

Zaffarano, B. (2010) Ferrets: examination and standards of care. *Journal of Exotic Pet Medicine* **19**, 73-81

Supporting Information

The following supporting information is available for this article:

Table S1. Reasons ferrets were excluded from this study. A total of 57 ferrets were excluded